

# Infiltration of Fibrous Preforms by a Pure Metal: Part III. Capillary Phenomena

A. MORTENSEN and T. WONG

Infiltration experiments on aluminum cast into SAFFIL alumina fiber preforms containing a silica binder and of fiber volume fraction varying from 10 to 25 pct are reported. Data are compared with the theory presented in Part I and used to characterize wettability of the preforms by plotting the infiltrated length of composite divided by the square root of time as a function of applied pressure. The intercept of the resulting curves with the abscissa axis is shown to be a measurement of the capillary pressure needed to fully infiltrate the fiber preforms. Resulting experimental values of this capillary pressure are then used with Brunauer, Emmett, and Teller (BET) adsorption isotherm measurements of the preform's specific surface to derive an apparent wetting angle of the fibers by aluminum during infiltration. In this manner, the effective wetting angle of pure aluminum on the alumina/silica fibers is found to be  $106 \pm 5$  deg, independent of fiber preform temperature. We also propose a mechanism for preventing preform compression during infiltration.

## I. INTRODUCTION

IN two preceding publications,<sup>[1,2]</sup> a theoretical analysis of the infiltration of fibrous preforms by molten metal was presented and compared with experimental data. It was found that the capillary pressure drop at the infiltration front can be estimated on a plot of  $L/\sqrt{t}$  (defined as  $\psi$ ) vs the applied pressure  $\Delta P_T$ , driving the metal into the preform, where  $L$  is the metal front position and  $t$  is time. An example is given in Figure 6 of Reference 2.

Use of the capillary pressure drop to estimate wettability is to be contrasted with usual techniques which measure a wetting angle using the sessile drop technique or a variety of dipping experiments. These and, in particular, the sessile drop technique are well established and easy to interpret. However, there can be major drawbacks in using their results to model infiltration, primarily because of the requirement for a smooth substrate and the static nature of these experiments. In this work, these drawbacks are overcome by using the results of dynamic infiltration experiments, in which a capillary pressure is estimated directly on fiber preforms of engineering interest. The resulting estimate can be converted to an apparent wetting angle which is characteristic of the highly transient type of wetting encountered in casting metal matrix composites.

In the following, data for the infiltration of alumina fiber preforms by liquid aluminum are presented with a wide range in the variation of the fiber volume fraction (10 to 25 pct) and initial temperature (313 to 558 K). These data are compared with the theory presented in Reference 1 and are also used to estimate the effective wetting angle of aluminum on these preforms during infiltration.

## II. EXPERIMENTAL PROCEDURE

Materials and procedures used in this study were similar to those reported in Reference 2. In brief, molten 99.99 pct pure aluminum was forced under applied pressure  $\Delta P_T = P_0 - P_g$  into preforms of SAFFIL\* alumina

---

\*SAFFIL is a trademark of ICI Americas, Inc., Wilmington, DE.

---

fibers, where  $P_0$  is the pressure at the preform entrance applied *via* pressurized nitrogen onto the metal. The term  $P_g$  is pressure in the gas phase initially present in the preform, equal to 1 atmosphere in this work. The fibers were oriented randomly within a plane perpendicular to the infiltration direction, and cohesion of the preform was obtained with a silica binder. Figure 1 is a scanning electron micrograph of the initial preform structure, where the binder is visible as a rugged phase covering part of the fiber surface. The preforms were obtained from various sources, and the fiber volume fractions varied from 10 to 25 pct.

The position of the metal infiltration front was recorded dynamically during each infiltration experiment.<sup>[2]</sup> The value of  $\psi$  was then taken from the slope of the linear portion of plots of  $L$  vs  $\sqrt{t}$ , as described in Reference 2. The metal temperature was initially at  $953 \pm 5$  K, and the initial fiber temperature  $T_f$  was controlled independently between 313 and 558 K  $\pm 5$  K. The temperature  $T_f$  was selected to satisfy the dual requirements of (1) infiltration of a measurable length of preform before external cooling caused excessive solidification at the preform entrance and (2) full pressurization of the apparatus before the entire preform was infiltrated.

Metallographic procedures are described in Reference 2. The specific surface of the preforms was obtained from Brunauer, Emmett, and Teller (BET) adsorption isotherm measurements of the preforms after degassing at 473 K for more than an hour immediately before each series of measurements. Each BET data point represents the average of at least four measurements preceded by one measurement which was discarded. Data for 24 and 25 vol pct fiber are combined, because these preforms were prepared from the same batch of fibers using an

---

A. MORTENSEN, ALCOA Assistant Professor, is with the Department of Materials Science and Engineering, Massachusetts Institute of Technology, Cambridge, MA 02139. T. WONG, formerly Undergraduate Student with the Department of Materials Science and Engineering, Massachusetts Institute of Technology, is a Consultant with Oliver, Wyman and Company, New York, NY 10036.

Manuscript submitted November 27, 1989.

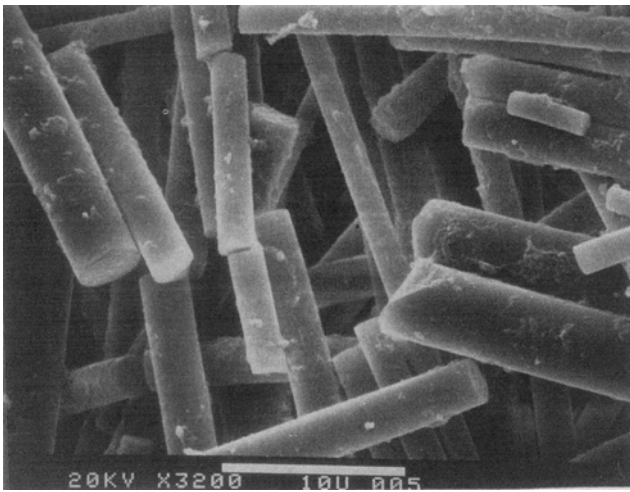


Fig. 1—Scanning electron micrograph of a SAFFIL fiber preform.

identical procedure and binder amount. The permeability to water of the preforms was measured as described in Reference 2.

### III. EXPERIMENTAL RESULTS

Plots of  $\psi^2$  as a function of  $\Delta P_T$  are given in Figure 2 for the various preforms investigated here. It is seen that the data fall roughly on a straight line, drawn on the figures from a least-squares regression of the data. At values of applied pressure higher than for data plotted in Figure 2, the infiltration kinetics measured by  $\psi$  were frequently below values predicted by the trend of data observed plotted in Figure 2. After infiltration, it was observed that in these samples, the preforms had deformed by compression against their upper support, an effect never observed with samples infiltrated at lower pressures and plotted in Figure 2. It is thus evident that at pressures above about 1.5 MPa for 10 vol pct fibers

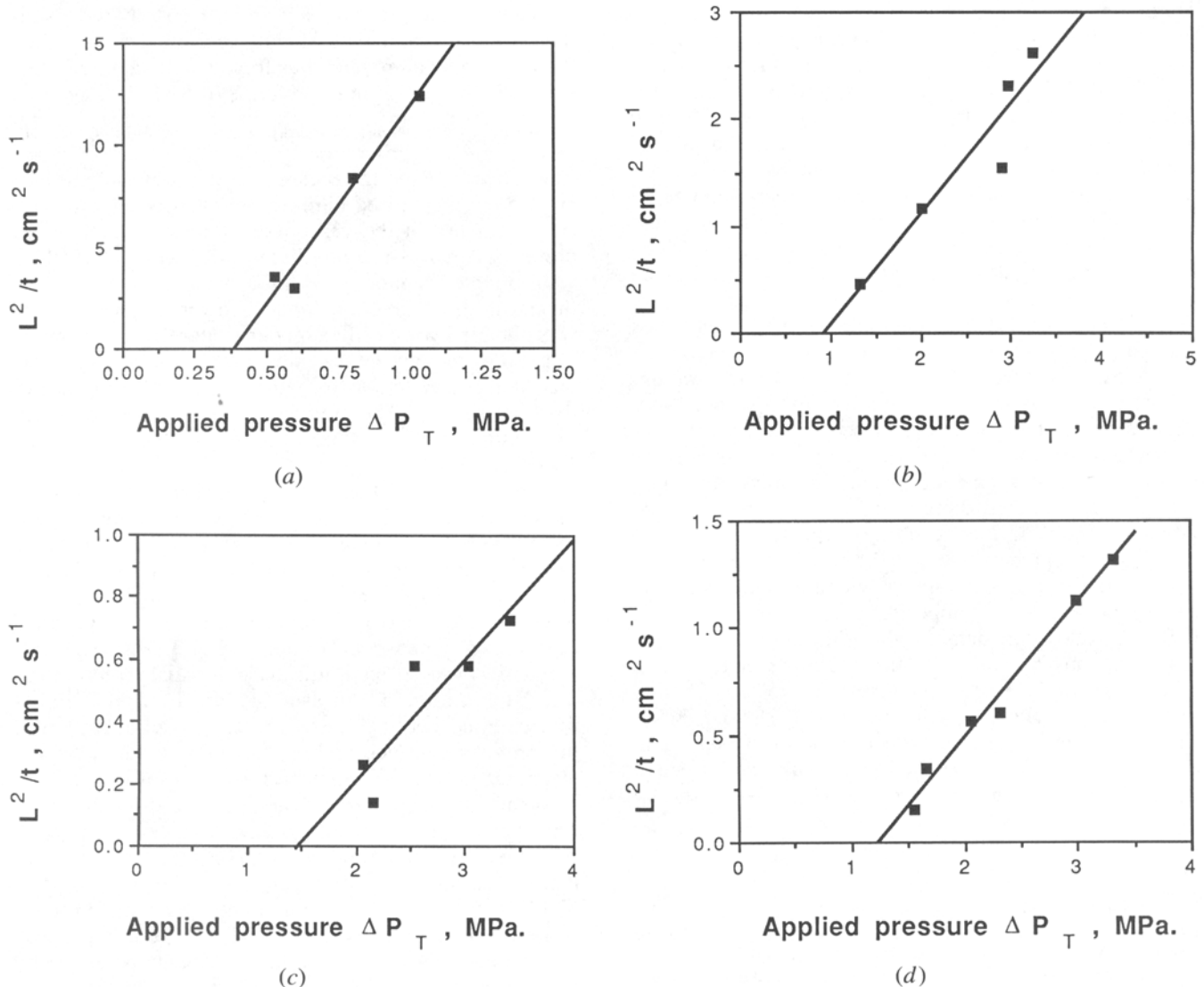


Fig. 2—Experimental plots of  $\psi^2$  as a function of applied pressure  $\Delta P_T$  for fiber volume fractions and initial temperatures of (a) 10 pct, 313 K; (b) 20 pct, 453 K; (c) 25 pct, 528 K; and (d) 25 pct, 558 K. The straight line on each graph is a least-squares fit through the data.

and 4 MPa for 20 to 25 vol pct fibers, the preforms may be compressed, resulting in an increased volume fraction fiber. This, in turn, lowers the rate of infiltration and causes a deviation from curves plotted in Figure 2. The high-pressure data, therefore, were discarded.

The infiltration front of the samples was smooth on a macroscopic scale but microscopically irregular (Figure 3). At the very tip of the infiltration front, the metal first infiltrated the larger pores of the preform. Full infiltration was observed a short distance therefrom, representing less than 5 pct of the total length of the samples.

Specific surfaces are given in Table I. They vary by about 10 pct between samples taken from a given preform, more than within each series of measurements on an individual sample (less than 5 pct). Therefore, some of the variation from one sample to another is because of variations in binder content, fiber volume fraction, *etc.* Thus, data in Table I are averages for each preform. Also shown in Table I are values of the surface area of fibers per unit volume pore in the preform (or metal matrix in the composite),  $S_f$ .

Values of the permeability of the various preforms measured by flowing water are given in Figure 4, and are seen to agree well with Eq. [18] of Sangani and Acrivos<sup>[3]</sup> (Eq. [26] in Reference 1).

#### IV. DISCUSSION

##### A. Method of Data Analysis

The forces which oppose flow of the metal into the preform manifest themselves by a pressure differential

$\Delta P_\mu$  between the pressure  $P_0$  at the preform entrance ( $x = 0$ ) and that in the metal at any point just behind the infiltration front,  $P_t$ . The pressure  $P_t$  differs from the pressure within the gaseous phase in the preform,  $P_g$ , because of capillary forces which either oppose or drive flow of the metal by creating a pressure differential  $\Delta P_\gamma = P_t - P_g$  across the infiltration front.

In Reference 1, a method was presented for calculating the kinetics of infiltration as a function of  $\Delta P_\mu$ . It was assumed that the infiltration front is planar (*i.e.*, "slug flow") and located at  $x = L$ . It was then shown that for unidirectional adiabatic infiltration under constant applied pressure and with no metal superheat,  $\psi^2$  is proportional to  $\Delta P_\mu$  (Eq. [47] of Reference 1, with  $\chi_s = 0$ ). Because

$$\Delta P_T = \Delta P_\gamma + \Delta P_\mu \quad [1]$$

a plot of  $\psi^2$  vs  $\Delta P_T$  can be used to estimate  $\Delta P_\gamma$  if  $\Delta P_\gamma$  is independent of applied pressure. In practice, however, the assumptions of no metal superheat and of slug flow are only approximately obeyed.

Infiltration with zero metal superheat is not practical, and the effect of small but finite superheat on linearity of the  $\psi^2$  vs  $\Delta P_T$  curve must be examined before extrapolating experimental data as a straight line to read  $\Delta P_\gamma$ . To this end, the predicted curve between  $\psi^2$  and  $\Delta P_\mu$  was calculated according to Eqs. [47], [51], [58], and [60] of Reference 1. Results for the present experiments are plotted in Figure 5. It is seen that the model predicts that  $\psi^2$  is roughly proportional to  $\Delta P_\mu$ . The superheat used in the present experiments, therefore, does

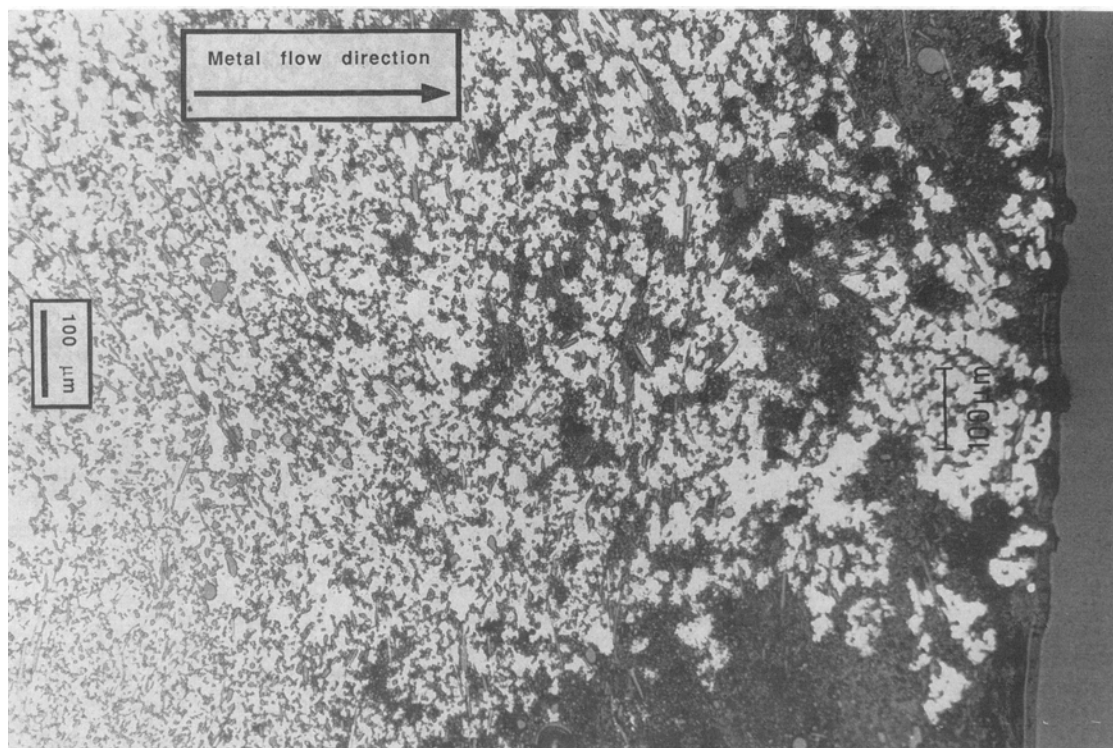


Fig. 3—Optical micrograph of the infiltration front of a sample infiltrated at  $V_f = 24$  pct,  $T_f = 558$  K, and  $\Delta P_T = 3.5$  MPa. The total infiltrated composite length is 38.5 mm. The arrow indicates the direction of infiltration.

Table I. Specific Surface of Fiber Preforms

Fiber Volume Fraction	Specific Surface (m <sup>2</sup> · g <sup>-1</sup> )	Average Specific Surface (m <sup>2</sup> · g <sup>-1</sup> )	S <sub>f</sub> m <sup>2</sup> Fiber Surface/m <sup>3</sup> Voids
10 pct	3.3	3.45	1.26 × 10 <sup>6</sup>
	3.6	—	—
20 pct	3.8	4.1	3.41 × 10 <sup>6</sup>
	4.4	—	—
24 and 25 pct	3.9	4.2	4.39 × 10 <sup>6</sup> (for V <sub>f</sub> = 24 pct)
	4.4	—	4.58 × 10 <sup>6</sup> (for V <sub>f</sub> = 25 pct)
	4.2	—	—

not invalidate extrapolation of data in Figure 2 to estimate ΔP<sub>γ</sub>.

The assumption of slug flow is always violated to some extent, because the metal infiltrates the preform over a range of pressures. For a preform that is poorly wetted by the metal and neglecting percolation effects, this range of pressures will extend from the capillary pressure needed to infiltrate the widest pores to that required for the metal to penetrate the finest interstices of the preform (a pressure that is infinite if two smooth cylindrical fibers touch along their length<sup>[4]</sup>). This phenomenon is discussed in several reviews of the capillarity of porous media.<sup>[5-8]</sup> Thus, the first drainage curve of gas in the preform by a metal is never a simple step function but instead rises gradually from V<sub>m</sub> = 0 to V<sub>m</sub> = 1 - V<sub>f</sub> over a range of applied pressures ΔP<sub>T</sub> if V<sub>m</sub> is the volume fraction of metal in the resulting composite.

Consider the unidirectional adiabatic infiltration under constant applied pressure ΔP<sub>T</sub> of a fiber preform by pure metal with no superheat in the metal. Infiltration takes place over a range of capillary pressures varying from ΔP<sub>γ,1</sub>, the pressure for penetration of the largest pores of the preform, up to ΔP<sub>γ,2</sub>, the pressure for infiltration of all but perhaps the very finest pores left in the preform<sup>[4]</sup> (a condition deemed as "full infiltration"). It is clear that for a portion of the composite to be fully infiltrated, ΔP<sub>T</sub> > ΔP<sub>γ,2</sub> is a prerequisite. When this is the case, all equations of Reference 1 are valid within the

fully infiltrated portion of the composite. Downstream, within the partially infiltrated composite, the metal pressure P ranges from P<sub>g</sub> + ΔP<sub>γ,1</sub> to P<sub>g</sub> + ΔP<sub>γ,2</sub> and fluid flow is more complex than in the case of slug flow, because the continuity equation (Eq. [30] of Reference 1) becomes

$$-\frac{\partial v_o}{\partial x} = \frac{\partial V_m}{\partial t} \quad [2]$$

for unidirectional flow, where v<sub>o</sub> is the metal superficial velocity and t is time. Also, the permeability K (in Darcy's law, Eq. [29] of Reference 1) is a function of both V<sub>m</sub> and of the volume fraction and shape of solid metal formed by cooling at the fibers.

If it is assumed that V<sub>m</sub> is a hysteresis function<sup>[8]</sup> of pressure (i.e., a function of infiltration history but not infiltration rate) and that the permeability K is a hysteresis function of V<sub>m</sub> during infiltration (even in the presence of solid metal forming at the infiltration front), then it is known that the fluid-flow problem of infiltration under constant applied pressure can still be solved using the Boltzmann transformation.<sup>[7-10]</sup> Therefore, if x = L<sub>1</sub> is used to designate the position of the very first metal to enter the preform (where P = P<sub>g</sub> + ΔP<sub>γ,1</sub>) and x = L<sub>2</sub> is used to designate the position of the front of full infiltration of the composite (where P = P<sub>g</sub> + ΔP<sub>γ,2</sub>), then both L<sub>1</sub> and L<sub>2</sub> move as ψ<sub>i</sub>√t, where ψ<sub>i</sub> (i = 1, 2) are constants which depend on process parameters.

During the experiments, it was reasonable to assume that the sensor used to detect the position of the metal front during infiltration established electrical contact with the aluminum where a given pressure was reached within the metal. The position of the metal as a function of time, therefore, should be proportional to √t, as observed, regardless of the value of the contact pressure. The final position of the infiltrated front measured by the sensor compared very closely to the final length of the composite. Metallographic examination of the cast composites (Figure 3) consistently revealed that only a small portion of the cast samples was porous. Because of the countergravitational direction of infiltration, no decrease in the length of porous composite was expected. We, therefore, conclude that L<sub>1</sub> and L<sub>2</sub> are very close to one another in the present samples and to the infiltration length measured by the sensor.

That portion of the composite behind L<sub>2</sub> can be treated as a composite of length L<sub>2</sub> infiltrated under slug-flow conditions with ΔP<sub>γ</sub> = ΔP<sub>γ,2</sub>. A plot of ψ<sub>2</sub><sup>2</sup> as a function of applied pressure ΔP<sub>T</sub> is, therefore, a straight line when

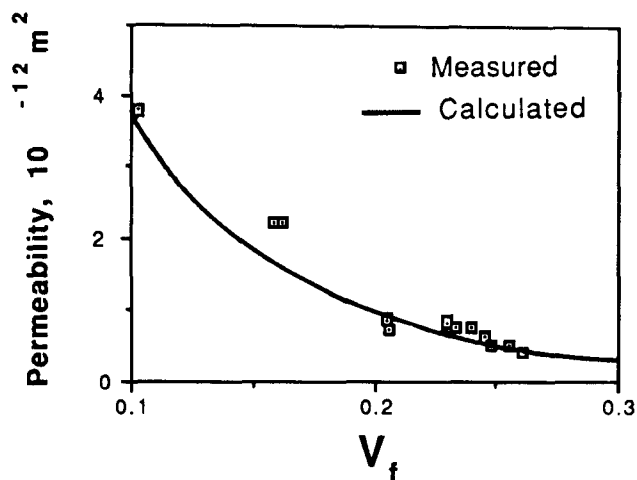


Fig. 4—Comparison of permeability measured by flowing water through the preforms with the prediction by Eq. [18] of Sangani and Acrivos.<sup>[3]</sup>

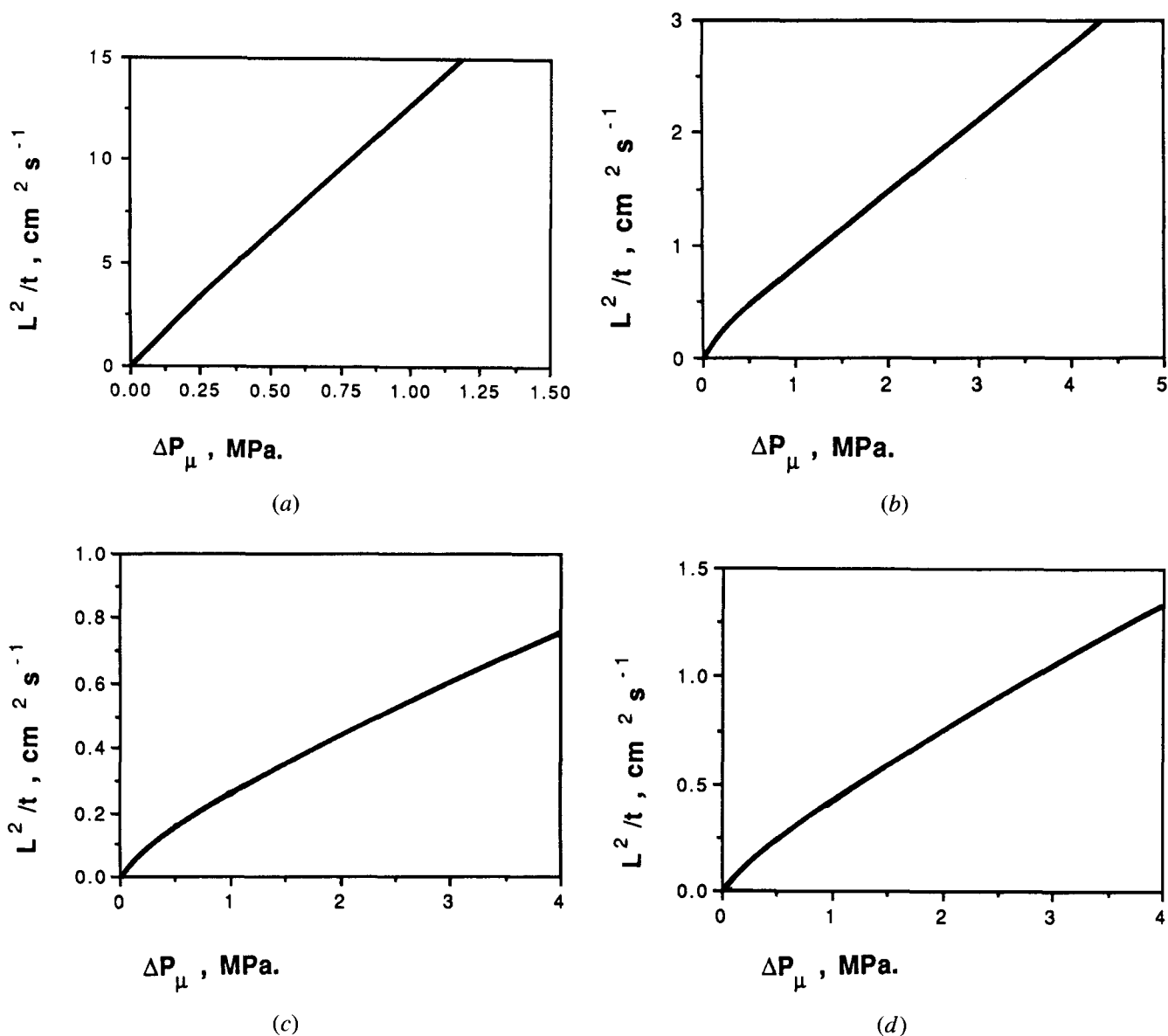


Fig. 5—Calculated plots of  $\psi^2$  as a function of the pressure differential between preform entrance and metal at the infiltration front  $\Delta P_\mu$  for fiber volume fractions and initial temperatures of (a) 10 pct, 313 K; (b) 20 pct, 453 K; (c) 25 pct, 528 K; and (d) 25 pct, 558 K.

there is no metal superheat. However, the same could not be said of  $\psi_1$  or  $\psi$  for any point within the partially infiltrated region of the composite, even though these points also move proportionally to  $\sqrt{t}$ . It is deduced that in these experiments, the intercepts of the straight lines plotted in Figures 2(a) through (d) provide estimates of  $\Delta P_{\gamma,2}$  which is the capillary pressure needed for full infiltration.

### B. Discussion of Data

Approximate calculated slopes of  $\psi^2$  vs pressure were computed using linear regression of calculated points used in plotting Figures 5(a) through (d) and Figure 7 of Reference 2. Results are given in Table II and compared with experimental data plotted in Figure 2 and Figure 6 of Reference 2. The predicted and measured slopes of  $\psi^2$  vs  $\Delta P_\mu$  compare reasonably well, considering that they

follow one another over a range covering 1-1/2 orders of magnitude. The predicted values of  $\psi$  are systematically lower than measured values, and the discrepancy increases as  $T_f$  decreases. All properties used in the constants are well known (in particular, because the metal temperature within the composite is fixed at its melting point), and the expression of Sangani and Acrivos<sup>(3)</sup> for the permeability of fiber preforms is reasonably accurate over a wide range of fiber volume fractions (Figure 4). The reason for the discrepancy, therefore, must lie with the assumed effect of solid metal on permeability during infiltration. As seen in Figure 1, the alumina fibers are not regularly distributed in the preforms; instead, they are bundled together in some areas, while they leave relatively wide channels in others. In Reference 1, to calculate permeability with solid metal, it was assumed that solidification effected an increase in apparent diameter of fibers located on a regular square grid. If solid metal

does indeed deposit as a sheath on the fibers, then the model should overestimate the decrease in preform permeability with solidification. This is because the largest channels, through which most metal flows, are not as greatly affected by solid metal as the rest of the preform. This agrees with data reported in Reference 2 and in this paper. Also, the greater the volume solid metal formed per fiber, the more pronounced this effect. Hence, the discrepancy between actual and predicted permeability should increase with decreasing fiber preform temperature  $T_f$ , which agrees with the trend observed in Table II. The systematic error, however, is small compared to the wide range of variation of preform permeability with increasing fraction solid metal.

Based on the discussion in Section IV-A, it is concluded from data in Figure 2 and in Figure 6 of Reference 2 that the total capillary pressure drop  $\Delta P_{\gamma,2}$  at the infiltration front is approximately constant within each series of experiments (otherwise deviations from linearity would be observed in the plots). It is also concluded that uncertainty in the resulting measurement of  $\Delta P_{\gamma,2}$  mostly emanates from experimental scatter rather than from 20 K of superheat (Figure 5) or the small difference between  $L_2$  and  $L_1$  (Figure 3).

The total capillary pressure drop,  $\Delta P_{\gamma,2}$ , corresponds to infiltration of nearly all the pores in the preform (Figure 3). Application of the results of Reference 4 is then legitimate if we ignore energy losses connected with irreversibility in the movement of metal at the infiltration front. We, therefore, write:

$$\Delta P_{\gamma} = -S_f \sigma_{LA} \cos \theta \quad [3]$$

where  $\theta$  is the contact angle of the liquid metal on the solid substrate (the fiber in this case),  $\sigma_{LA}$  is the liquid metal surface energy, and  $S_f$  is the surface area of interface per unit volume metal matrix. Using the measure of  $\Delta P_{\gamma}$  from the curves in Figure 2, values of  $S_f$  from Table I, and  $\sigma_{LA} = 0.914 \text{ J} \cdot \text{m}^{-2}$ , the surface tension of liquid aluminum at its melting point,<sup>[11]</sup> a value for the apparent contact angle  $\theta$  during infiltration was calculated (Table III). It is seen that the value of  $\theta$  is relatively constant for all series of experiments at  $106 \pm 5$  deg. Using  $\sigma_{LA} = 0.865 \text{ J} \cdot \text{m}^{-2}$ , a slightly different value used by Laurent *et al.* for pure aluminum at its melting point,<sup>[12]</sup> one obtains  $\theta = 108 \pm 5$  deg.

Comparison to existing data on the wetting of alu-

**Table II. Comparison of Calculated and Measured Values of the Slope of  $\psi^2$  vs Applied Pressure (from Figures 2 and 5)**

$V_f$	$T_f$ (K)	Calculated Slope (Figure 5) ( $\times 10^4 \text{ m}^2 \text{ s}^{-1} \text{ Pa}^{-1}$ )	Slope of Line through Experimental Data (Figure 2) ( $\times 10^4 \text{ m}^2 \text{ s}^{-1} \text{ Pa}^{-1}$ )
0.10	313	13	19
0.20	453	0.68	1.1
0.24*	558	0.51	0.74
0.25	528	0.18	0.39
0.25	558	0.32	0.59

\*From data reported in Ref. 2.

**Table III. Wettability Measurements**

$V_f$	$T_f$ (K)	$\Delta P_{\gamma}$ (Figure 2) (MPa)	$\theta$ (Eq. [3]) (Deg)
0.1	313	0.39	110
0.2	453	0.91	107
0.24	558	0.85*	102
0.25	558	1.2	107
0.25	528	1.5	111

\*From Fig. 6 of Ref. 2.

minum on alumina<sup>[13-20]</sup> shows that our value of  $\theta$ , about 106 deg, differs significantly from that of a drop of aluminum on alumina at 933 K in the presence of oxygen, where  $\theta$  is about 160 deg. On the other hand, it agrees very well with recent data by Laurent *et al.*<sup>[12]</sup> who found  $\theta = 103 \pm 5$  deg at 933 K when oxygen partial pressures were low enough to suppress the oxide skin which normally covers molten aluminum and influences the wetting angle. Further, in that our apparent contact angle is independent of initial fiber temperature, our data agree with the low sensitivity of  $\theta$  to temperature found by Laurent *et al.* The most likely explanation of this agreement is that there is no oxide layer covering the metal as it infiltrates the preform because of the "skimming" action of the fibers that was first described by Cappleman *et al.*<sup>[21]</sup> With  $\sigma_{LA} = 1.050 \text{ J} \cdot \text{m}^{-2}$ , as given by Delannay *et al.*<sup>[22]</sup> for aluminum free of surface oxide, we find  $\theta = 104 \pm 4$  deg which is even closer to the result of Laurent *et al.*'s measurements. However, the presence of silica in both the fiber and the binder of our preforms limits the validity of the comparison to data of Laurent *et al.* which were collected on pure sapphire.

It must be borne in mind that the wetting situation of interest here is fundamentally different from that used in previous experiments on wetting of aluminum on alumina. When molten aluminum contacts the fibers at the infiltration front, the fibers are significantly below the melting point of the metal and there is rapid exchange of heat between fibers and metal. This results in undercooling and partial solidification of the metal immediately after contact is established with the fibers so that the wetting is transient, whereas in experiments of Laurent *et al.* and other researchers, contact angle measurements are from static experiments close to equilibrium conditions. In particular, given the wide range of variation in fiber temperature, the relative independence of  $\theta$  from  $T_f$  is surprising. This is indicative either of a constant temperature at the infiltration front, regardless of the initial fiber temperature  $T_f$ , or of a wetting angle that is independent of temperature.

Another surprising observation is that the preforms were only compressed during infiltration at relatively high applied pressures. Compression tests on the preforms<sup>[23]</sup> indicated that appreciable strain was imposed on the preforms under a compressive stress within the range of applied pressures used here. Analysis of the problem<sup>[24]</sup> indicates that in adiabatic infiltration, the preforms are compressed under a stress equal to the applied pressure and this should result in significant deviations from the linear portions of the  $\psi^2$  vs  $\Delta P_T$  plots for far lower values

of  $\Delta P_7$ . We propose that in the very first phase of the infiltration process, while the applied pressure is lower than the nominal value of the experiment, metal penetrates a short distance into the preform without significantly compressing it. Some metal then solidifies at the mold wall and anchors the fiber preform there. This anchor point at the preform entrance mechanically resists subsequent compression of the preform while the applied pressure rises and reaches its nominal value. This effect could explain the fact that fiber preform compression is appreciable only at a much higher value of applied pressure than is predicted on the basis of preform compressibility alone.

## V. CONCLUSIONS

1. Interpretation of infiltration data in terms of a capillary pressure drop  $\Delta P_\gamma$  at the infiltration front, deduced from measurements of infiltration kinetics with varying applied pressure, allows for a novel method of characterizing the wettability of fibrous preforms by molten metal during infiltration.
2. The influence of process parameters on infiltration kinetics is well predicted by the theoretical analysis presented in Reference 1. Preform permeability in the presence of solid metal is somewhat underestimated by the model, however. This slight but systematic deviation is interpreted to result from uneven fiber packing which causes solid metal forming on the fibers to leave the largest pores of the preform relatively unperturbed.
3. Using a molten aluminum surface tension of  $0.914 \text{ J} \cdot \text{m}^{-2}$  and ignoring irreversible energy losses in wetting of the preform by the metal, measured capillary pressure data yield an effective wetting angle of pure aluminum on the alumina/silica fibers of  $106 \pm 5$  deg, independent of initial fiber temperature.
4. Preform compression during infiltration was much less than expected for adiabatic infiltration. It is proposed that this is due to metal solidification at the mold wall in the initial stage of infiltration.

## ACKNOWLEDGMENTS

Funding of this work was by the Innovative Science and Technology Division of the Strategic Defense Initiative Office through the Office of Naval Research, Contract No. N00014-85-K-0645, under the supervision of Dr. S.G. Fishman. Discussions with Professor

Merton C. Flemings, Dr. Lawrence J. Masur, Dr. James A. Cornie, Ms. Tamala Fletcher, and Ms. Véronique J. Michaud and helpful comments from the reviewers of this article are gratefully acknowledged. Our grateful appreciation is also extended to students in our research group who assisted with the experimental work, to Mr. Jared Sommer for the BET measurements, and to Ms. Raquel D'Oyen for optical metallography. We thank Thermal Ceramics Inc. and the General Motors Corporation for donating fiber preforms used in this work.

## REFERENCES

1. A. Mortensen, L.J. Masur, J.A. Cornie, and M.C. Flemings: *Metall. Trans. A*, 1989, vol. 20A, pp. 2535-47.
2. L.J. Masur, A. Mortensen, J.A. Cornie and M.C. Flemings: *Metall. Trans. A*, 1989, vol. 20A, pp. 2549-57.
3. A.S. Sangani and A. Acrivos: *Int. J. Multiphase Flow*, 1982, vol. 8, pp. 193-206.
4. A. Mortensen and J.A. Cornie: *Metall. Trans. A*, 1987, vol. 18A, pp. 1160-63.
5. N.R. Morrow: *Ind. Eng. Chem.*, 1970, vol. 62 (6), pp. 32-56.
6. W.G. Anderson: *J. Pet. Technol.*, Oct. 1987, pp. 1283-1300.
7. D. Hillel: *Soil Water—Physical Principles and Processes*, Academic Press, New York, NY, 1971, pp. 255-58 and pp. 103-27.
8. E.E. Miller and R.D. Miller: *J. Appl. Phys.*, 1956, vol. 27, pp. 324-32.
9. J.R. Philip: *Soil Sci.*, 1957, vol. 84, pp. 257-64.
10. R.D. Jackson: *Soil Sci. Soc. Am. Proc.*, 1963, vol. 27, pp. 123-26.
11. *Smithells Metals Reference Book*, 6th ed., Butterworth's, London, 1983, p. 14.7.
12. V. Laurent, D. Chatain, C. Chatillon, and N. Eustathopoulos: *Acta Metall.*, 1988, vol. 36, pp. 1797-1803.
13. R.D. Carmahan, T.L. Johnston, and C.H. Li: *J. Am. Ceram. Soc.*, 1958, vol. 41 (9), pp. 343-47.
14. S.M. Wolf, A.P. Levitt, and J. Brown: *Chem. Eng. Prog.*, 1966, vol. 63 (3), pp. 74-78.
15. J.J. Brennan and J.A. Pask: *J. Am. Ceram. Soc.*, 1968, vol. 51 (10), pp. 569-73.
16. J.A. Champion, B.J. Keene, and J.M. Sillwood: *J. Mater. Sci.*, 1969, vol. 4, pp. 39-49.
17. N. Mori, H. Sorano, A. Kitahara, K. Oogi, and K. Matsuda: *J. Jpn. Inst. Met., Sendai*, 1983, vol. 47 (12), pp. 1132-39.
18. W. Dawihl and H. Federmann: *Aluminium (Duesseldorf)*, 1974, vol. 50, pp. 574-77.
19. H. John and H. Hausner: *J. Mater. Sci. Lett.*, 1986, vol. 5, pp. 549-51.
20. L. Coudurier, J. Adorian, D. Pique, and N. Eustathopoulos: *Rev. Int. Hautes Temp. Refract.*, 1984, vol. 21, pp. 81-93.
21. G.R. Cappleman, J.F. Watts, and T.W. Clyne: *J. Mater. Sci.*, 1985, vol. 20, pp. 2159-68.
22. F. Delannay, L. Froyen, and A. Deruyttere: *J. Mater. Sci.*, 1987, vol. 22, pp. 1-16.
23. T. Wong: Massachusetts Institute of Technology, Cambridge, MA, unpublished research, 1988.
24. A. Mortensen: Massachusetts Institute of Technology, Cambridge, MA, unpublished research, 1988.